

TMT-Based Quantitative Proteomics Revealed the Antibacterial Mechanism of Cinnamaldehyde against MRSA

Xiaohui Chen, Panpan Liu, Jingge Wang, Xiaoqiang He, Jianchong Wang, Haorong Chen, and Guiqin Wang*

Cite This: <https://doi.org/10.1021/acs.jproteome.4c00520>

Read Online

ACCESS |



Metrics & More



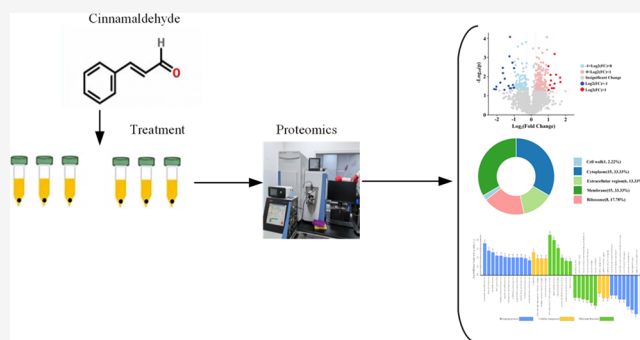
Article Recommendations



Supporting Information

ABSTRACT: Natural plant extracts have demonstrated significant potential in alternative antibiotic therapies. Cinnamaldehyde (CA) has garnered considerable attention as a natural antibacterial agent. In this study, Tandem mass tag (TMT) quantitative proteomics combined with Western blot and RT-qPCR methods were employed to explore the antibacterial mechanism of CA against Methicillin-Resistant *Staphylococcus aureus* (MRSA) at the protein level. The results showed that a total of 254 differentially expressed proteins (DEPs) were identified in the control group and CA treatment group, of which 161 were significantly upregulated and 93 were significantly downregulated. DEPs related to nucleotide synthesis, homeostasis of the internal environment, and protein biosynthesis were significantly upregulated, while DEPs involved in the cell wall, cell membrane, and virulence factors were significantly downregulated. The results of GO and KEGG enrichment analyses demonstrated that CA could exert its antibacterial effects by influencing pyruvate metabolism, the tricarboxylic acid (TCA) cycle, teichoic acid biosynthesis, and the *Staphylococcus aureus* (*S. aureus*) infection pathway in MRSA. CA significantly inhibited the expression of recombinant protein MgrA ($p < 0.05$), significantly reduced the mRNA transcription levels of *mgrA*, *hla*, and *sdrD* genes ($p < 0.05$), and thermostability migration assays demonstrated that CA can directly interact with MgrA protein, thereby inhibiting its activity. These findings suggest that CA exerts its antibacterial mechanism by regulating the expression of related proteins, providing a theoretical basis for further development of clinical applications of antimicrobial agents derived from natural plant essential oils in the treatment of dairy cow mastitis.

KEYWORDS: TMT-based proteomic analysis, cinnamaldehyde, MRSA, antibacterial mechanism



1. INTRODUCTION

Mastitis is widely recognized as a prevalent and significant disease within the global dairy sector due to its profound implications for dairy cow productivity, welfare, health, and fertility.¹ *S. aureus* represents a significant pathogen contributing to bovine mastitis, and antibiotics remain the primary treatment for mastitis in dairy cows. However, with the widespread use of antibiotics, *S. aureus* has developed significant resistance and an immune response to these drugs. MRSA is resistant to most antibiotics due to the production of penicillin-binding protein 2a (PBP2a), which leads to a rapid decline in the efficacy of traditional antibiotics.² Currently, the eradication rate of antibiotic-resistant bacteria typically falls below 60%.³ Therefore, there is an urgent need to develop effective antimicrobial agents to combat and control the spread of *S. aureus*.

In the realm of alternative antibiotic treatments, natural plant extracts have shown considerable promise, particularly in the realm of dairy production, garnering increasing attention.⁴ Natural plant extracts are characterized by low toxicity and a reduced propensity for drug resistance. Their antibacterial

effects primarily manifest through disrupting bacterial cell membrane integrity, interfering with bacterial protein biosynthesis, and inhibiting intracellular DNA replication and repair.⁵ Natural bioactive substances, such as plant essential oils (PEOs), polyphenols, bacteriocins, and lipids, exhibit significant antibacterial activity. Among them, PEO is an oily liquid characterized by hydrophobicity, aromaticity, and volatility. Its chemical components mainly include aldehydes, phenols, alcohols, acids, ketones, terpenes, and aromatic compound,⁶ and their primary constituents exhibit a range of antibacterial targets, particularly affecting the cell wall and plasma membrane. Their lipophilic constituents facilitate penetration through bacterial and mitochondrial cell membranes, inducing cell wall degradation, cytoplasmic membrane disruption,

Received: June 28, 2024

Revised: August 16, 2024

Accepted: September 6, 2024

cytoplasmic coagulation, and reduction of intracellular ATP levels, consequently impairing cellular functions including membrane transport, energy production, and various other metabolic regulatory processes.^{7,8} Furthermore, compounds in EOs disrupt cell function by binding to DNA, RNA, and proteins, interfering with membrane proteins and initiating processes such as electron transfer and protein translocation. These actions collectively inhibit cell component synthesis and enzyme activity, resulting in bacterial lysis and death.^{9,10} The most active components of EOs are predominantly aldehydes and phenols, among which CA is an aromatic aldehyde. As the main component of cinnamon EO, CA has garnered significant attention due to its antibacterial properties.¹¹ CA exhibits natural antibacterial and antibiofilm properties.¹² CA has been reported to exhibit antibacterial activity against *Staphylococcus epidermidis*, drug-resistant *Aeromonas hydrophila*, enterohemorrhagic *Escherichia coli*, uropathogenic *Escherichia coli* (UPEC), *Streptococcus agalactiae*, and MRSA.¹³ CA typically induces biological effects, including abnormal cell membrane rupture in *S. aureus* and *Escherichia coli*, disruption of the cell membrane potential, and inhibition of ATP synthesis,¹⁴ effectively inhibits biofilm formation in *Streptococcus agalactiae* and significantly downregulates the transcription of the *pilA*, *pilB*, and *rogB* regulatory genes associated with pilus synthesis in *Streptococcus agalactiae*.¹⁵ CA can inhibit the biosynthesis of the bacterial cell wall; destroy the membrane structure and integrity; interfere with systems involved in energy production and the synthesis of structural components; inhibit bacteria, yeasts, and filamentous fungi; and eventually lead to cell lysis and death.¹⁶ Nevertheless, to the best of our knowledge, a thorough investigation into the specific mechanisms driving the overall impact of CA on MRSA remains incomplete. Hence, acquiring a profound comprehension of the interactions between CA and MRSA at the protein level will aid in elucidating the mechanisms of antimicrobial drugs. Thorough characterization of the interaction between antimicrobial agents and macromolecules is paramount for safe and effective utilization of these agents.

Proteomics can offer sophisticated insights into microbial biochemical reactions, facilitate elucidation of the molecular mechanisms by which antibacterial drugs inhibit pathogenic microorganisms, and represent the most potent approach for investigating the antibacterial mechanism of CA against MRSA. TMT is a quantitative protein technology that uses isotope labeling *in vitro*. It allows for a thorough evaluation of the effects of CA on the entire metabolism of MRSA cells by identifying proteins that are produced differently.¹⁷ Du et al. employed TMT proteomics analysis to uncover that the main antibacterial mechanism of trans-cinnamaldehyde against *Escherichia coli* encompasses aldehyde toxicity, acid and oxidative stress, disturbance of carbohydrate and energy metabolism, and disruption of protein translation.¹⁸ Fan et al., using TMT quantitative proteomics and nontargeted metabolomics, revealed that hexanal disrupts the structure and function of the *Vibrio parahaemolyticus* cell membrane, inhibits nucleotide metabolism, disrupts carbohydrate metabolism and the TCA cycle, and ultimately leads to bacterial growth inhibition and death.¹⁹ Deng et al., using TMT quantitative proteomics and multiple reaction monitoring (MRM) technology, revealed, based on protein level, that Aronia melanocarpa anthocyanins (AMAs) induced bacterial morphological changes and cell death by affecting *Escherichia coli* protein biosynthesis, DNA replication and repair, oxidative

stress response, and peptidoglycan biosynthesis.⁵ In addition, Yang et al. used TMT quantitative proteomics to reveal that the new antimicrobial peptide AMP-17 induces a range of complex biological reactions by affecting oxidative phosphorylation, RNA degradation, propionic acid metabolism, and fatty acid metabolism in *Candida albicans* and inhibits fungal growth by targeting multiple sites within *Candida albicans* cells.²⁰ In this study, TMT proteomics technology was utilized to analyze CA's impact on the expression of all proteins in MRSA cells. Gene Ontology (GO) annotation and Kyoto Encyclopedia of Genes and Genomes (KEGG) pathway enrichment analysis were utilized to assess differential protein enrichment pathways and subcellular localization. CA's effect on the activity of recombinant protein was detected by Western blot and thermostable migration assay, while CA's effect on the mRNA transcription levels of relevant genes was evaluated by RT-qPCR. This approach enables a deeper understanding of the mechanism of action of CA antibacterial drugs.

2. MATERIALS AND METHODS

2.1. Activation and Culture of Strains

MRSA strains were kept in freezer tubes with MH broth (Haibo Biological, Qingdao, China) supplemented with 80% (v/v) glycerol for an extended period of time at -80°C . The MRSA solution was streaked onto MH agar plates (Haibo Biological, Qingdao, China), and subsequently, a single colony was selected and cultured until reaching the logarithmic growth phase.

2.2. Protein Extraction and Quantification

The MRSA bacterial suspension cultured overnight was diluted to a concentration range of 10^6 to 10^8 CFU/mL. Subsequently, 1 mL of bacterial suspension without CA and 1 mL of bacterial suspension with CA at $1\times$ MIC were incubated in a temperature-controlled shaker (37°C , 220 rpm) for 8 h. Afterward, the bacterial precipitate was collected by centrifugation, and the cell precipitate was frozen in liquid nitrogen and stored at -80°C . Three samples were collected from each group for subsequent proteomics analyses. An appropriate amount of SDT Lysis Buffer cracking solution was added to each sample and then boiled for 3 min, followed by ultrasonic treatment. After centrifugation, the protein content was determined by using a Bicinchoninic acid (BCA) assay kit. Total protein from MRSA strains treated with either the control or CA medication was quantitatively analyzed using the BCA method and 15% SDS-PAGE gel electrophoresis.

2.3. Protein Digestion and TMT Labeling

A suitable quantity of protein samples was collected for enzymatic hydrolysis and subsequently subjected to desalting using a Thermo desalting spin column for the purpose of peptide quantification. The peptides from each sample were labeled in the same manner according to the instructions provided by the TMT labeling kit (Thermo Scientific, USA).

2.4. HPLC Fractionation and LC-MS/MS Analysis

The peptides that were labeled in each group were mixed in equal amounts, and the peptides that had been dried were separated by using the Vanquish Neo UHPLC system (Thermo Scientific). Afterward, the samples were gathered and combined into 10 fractions. The peptides from each fraction were dehydrated, rehydrated in a solution containing 0.1% formic acid (FA), and individually examined on the

instrument. The peptides were dissolved in a solution containing 0.1% FA, while the chromatographic column was equilibrated with a 96% aqueous solution containing 0.1% FA. The samples were injected onto the Trap Column (PepMap Neo 5 μm C18, 300 μm \times 5 mm, Thermo Scientific) by gradient separation using the chromatographic analysis column (μPAC Neo High Throughput column, Thermo Scientific). Following this, the peptides were subjected to separation and analysis utilizing an Orbitrap Astral mass spectrometer (Thermo Scientific). The ion source voltage was adjusted to 2.2 kV, while the primary mass spectrometer scanning range was defined as 380–980 m/z with a scanning resolution of 240,000. The secondary scanning resolution was configured at 80,000, and data acquisition was carried out through a data-dependent scanning protocol, maintaining consistent scanning procedures for both second-order and first-order mass spectrometry.

2.5. Database Retrieval

Use the CHIMERYs search engine on the Ardia Server within the Proteome Discoverer software (Thermo Scientific) to import the final LC–MS/MS RAW file into the database for retrieval. The tandem mass spectrum was matched against the *S. aureus* database (108516 sequences) and the reverse bait database. The primary query parameter is set to utilize trypsin/P as the cleavage enzyme, permitting a maximum of two missed cleavages. During the initial search, the allowed difference in mass for the precursor ion was set at 20 ppm. However, in the subsequent search, this tolerance was improved to 10 ppm. Additionally, the allowed difference in mass for the fragment ions was set at 0.02 Da. The quantification method used was TMT-6plex, and the false discovery rate (FDR) for identifying proteins and peptide spectrum matches (PSMs) was set at 0.1%. The threshold for determining significant changes is set at a fold change ratio of ≥ 1.5 or < 0.83 , in addition to a t test p -value less than 0.05.

2.6. Bioinformatics Analysis

Proteins were categorized based on these three aspects using GO annotations. KEGG functional enrichment analysis was then conducted using Fisher's exact test algorithm on the annotation results. Subsequently, the subcellular localization of proteins was forecasted using Wolfpsort software for subcellular localization prediction. Enrichment analysis results with a significance level of $p < 0.05$ were considered significant, with a smaller p -value indicating more substantial functional enrichment. Integration of protein–protein interaction (PPI) data from the STRING database with pathway–protein relationships facilitated prediction of the PPI network for DEPs. The network was selected and constructed by using the PageRank algorithm.

2.7. Expression and Purification of Recombinant Protein and Preparation of Polyclonal Antibody

A fragment of the *mgrA* gene was amplified by using genomic DNA extracted from MRSA, and the pET-28a(+)-*mgrA* recombinant plasmid was constructed by using seamless cloning. The recombinant plasmid pET-28a(+)-*mgrA* was then transformed into BL21 (DE3) through heat shock transformation to generate the recombinant strain BL21/pET-28a(+)-*mgrA*. Positive single colonies were identified and inoculated into LB liquid medium containing kanamycin resistance overnight. The prokaryotic expression of MgrA protein was induced at a low temperature overnight using a

final concentration of 0.05 mmol/L isopropyl β -D-thiogalactoside (IPTG). Subsequently, the MgrA protein was purified using the Ni-NTA protein purification method; the concentration of the substance was ascertained using the BCA technique. The purified MgrA protein was then sent to Chengdu Lilai Biomedical Experimental Center to prepare polyclonal antibodies.

2.8. Effect of CA on the Expression of Recombinant Protein

After being treated with different doses of CA overnight, the MRSA suspensions were subjected to centrifugation to gather the sediment. Afterward, the sediment was rinsed with PBS, and the bacterial suspension was reconstituted. Following the SDS-PAGE gel electrophoresis, the proteins were subsequently deposited onto a poly(vinylidene fluoride) (PVDF) membrane. The primary antibody used was anti-MgrA rabbit polyclonal antibody, while the secondary antibody employed was HRP-coupled goat antirabbit IgG. MgrA-specific bands' expression was detected by enhanced chemiluminescence (ECL).

2.9. Quantitative Real-Time PCR

The TRIzol technique was employed to extract RNA from both the control and the medication groups. Afterward, the RNA was converted into complementary DNA (cDNA) using the SPARKscript II All-in-One RT SuperMix for qPCR (with gDNA Eraser) reverse transcription kit, following the instructions. RT-qPCR primer sequences for *gyrB*, the internal reference gene, are provided in Table 1. RT-qPCR was

Table 1. RT-qPCR Primer Sequences

| primer name | primer sequences (5'–3') |
|----------------|------------------------------|
| <i>gyrB</i> _F | AGGCTCTGGAGAAATGAATG |
| <i>gyrB</i> _R | CAAATGTTTGGTCCGCTT |
| <i>sdrD</i> _F | GCAGATGGTGGCGAAGTTGACG |
| <i>sdrD</i> _R | CACTGTCTGAGTCTGAGTCGCTG |
| <i>mgrA</i> _F | ATCAAATGCATGAATGACTTTACCTAAT |
| <i>mgrA</i> _R | CCGAAGTCGATCAACGTGAAGTAT |
| <i>hla</i> _F | TATTAGAACGAAAGGTACCA |
| <i>hla</i> _R | ACTGTACCTTAAAGGCTGAA |
| <i>spa</i> _F | AGCGCTTTGGCTTGGGTCAT |
| <i>spa</i> _R | GAATCTCAAGCACCGAAAGCGGAT |

conducted using the 2 \times SYBR Green qPCR Mix (with ROX) reagent to detect alterations in the mRNA transcription levels of the relevant genes. The relative expression of genes was calculated using the $2^{-\Delta\Delta\text{CT}}$ method. Independent sample t tests were conducted by using SPSS 21.0, and GraphPad Prism software was utilized for graphical representation.

2.10. Effect of CA on the Thermal Stability of Recombinant Protein

The 50 μL portion of MgrA protein obtained through ultrasonic crushing and purification was transferred to a centrifuge tube. Various temperature gradient treatment groups were established with the addition of CA (1 \times MIC), along with a control group. Afterward, the samples were subjected to heating in a water bath for 10 min at various temperatures, cooled to room temperature for 3 min, centrifuged, and collected the supernatant. The expression of the MgrA protein was analyzed using SDS-PAGE gel electrophoresis.

3. RESULTS AND ANALYSIS

3.1. Identification of MRSA Total Protein

SDS-PAGE gel analysis revealed that the protein bands in both the control group (WLD19) and the CA treatment group samples are clear and consistent, indicating the absence of protein degradation or dispersion. Additionally, the parallelism of each lane indicates a high protein quality (Figure S1).

3.2. Protein Identification and DEPs Distribution and Analysis

To investigate the impact of CA on the protein expression of MRSA, TMT labeling and HPLC-MS/MS techniques were employed to quantitatively analyze the proteins in the CA treatment group and the control group. In total, 18343 peptides were detected (Table S1), and 2414 proteins were identified through comparison with the UniProt protein database (Table S2). 254 DEPs were identified in both the control group and the CA treatment group, comprising 161 significantly upregulated and 93 significantly downregulated DEPs. Significantly upregulated DEPs are denoted by red dots, significantly downregulated DEPs are denoted by blue dots, and gray spots represent non-DEPs (Figure 1A,B). Details of DEPs are listed in Table S3. Subcellular localization can locate DEPs in specific locations in cells, thus providing a research direction for understanding the mechanism of CA on MRSA. The results of subcellular localization analysis showed that 2.22% of the 254 DEPs were located in the cell wall, 33.33% in the cytoplasm, 13.33% in the outer membrane, 33.33% in the cell membrane, and 17.78% in the ribosome. These findings suggest that CA predominantly affects the cytoplasm and plasma membranes of MRSA (Figure 1C).

In this study, five proteins associated with the MRSA cell wall and cell membrane exhibited significant downregulation, showing reductions ranging from 0.30-fold to 2.04-fold. The results revealed that nine proteins associated with MRSA protein biosynthesis were significantly upregulated by factors ranging from 0.33-fold to 0.80-fold. Additionally, only small ribosomal subunit protein uS4 was significantly downregulated by 1.25-fold. The three DEPs (A0A7U4CHE4, A0A0E1VK28, and A0A9P2XZB2) associated with DNA replication were upregulated by 0.58-fold, 0.33-fold, and 0.59-fold. Furthermore, the factors associated with virulence and drug resistance in MRSA were downregulated by 0.47–1.18-fold after CA treatment (Table 2).

3.3. GO and KEGG Enrichment Analysis of DEPs

To examine the biological activities of distinct proteins between the control group and the CA treatment group, all DEPs identified in CA-treated MRSA were classified using secondary GO annotation (Figure 2A and Table S4). These annotation classifications suggest that DEPs are implicated in diverse arrays of biological processes, molecular functions, and cellular components. Regarding cellular components, upregulated DEPs were primarily localized within the cytoplasm and downregulated DEPs were primarily the riboflavin synthase complex and GMP reductase complex. Concerning molecular function, upregulated DEPs are predominantly involved in ribonucleoside binding and catalytic activity and downregulated DEPs were primarily symporter activity. Regarding biological processes, upregulated DEPs are primarily associated with metabolic processes and biosynthetic processes and downregulated DEPs were primarily iron–sulfur cluster assembly. Moreover, the prevalence of DEPs in metabolic

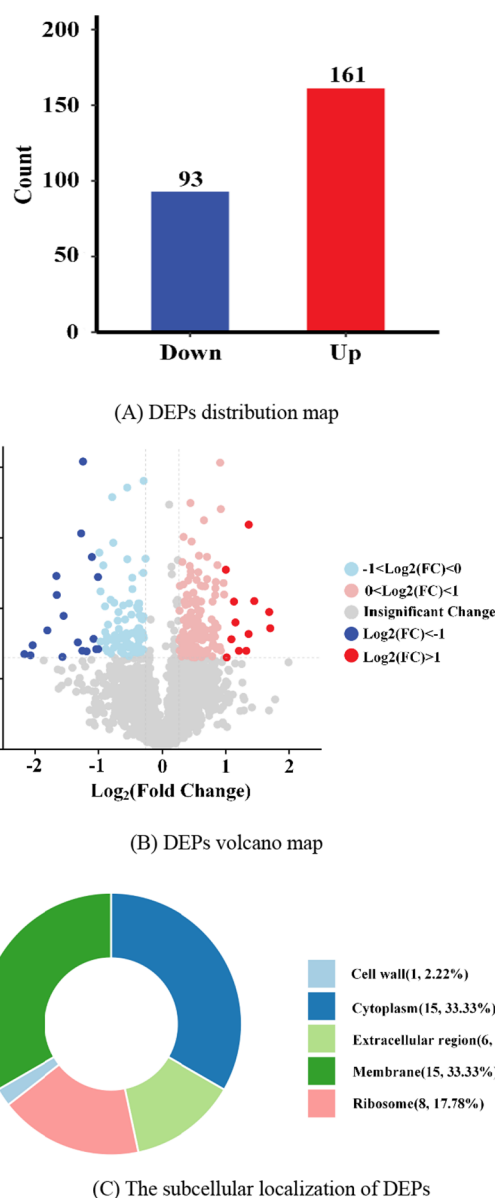


Figure 1. Statistical distribution of DEPs. Note: (A) Abscissa represents the type of DEPs, and the ordinate represents the total number of significant DEPs. (B) Abscissa represents the logarithmic transformation of FC, and the ordinate represents the negative logarithmic transformation of the p -value. Each point represents a protein: red points indicate significantly upregulated DEPs, with darker colors representing higher upregulation; blue points indicate significantly downregulated DEPs, with deeper colors representing higher downregulation; gray points represent non-DEPs. (C) Subcellular localization results for all DEPs.

processes and catalytic activity is notably high, indicating that DEPs generated by MRSA following CA treatment are crucial for metabolism. These findings indicate that these DEPs may have a significant effect on the mechanism of CA in combating MRSA.

Based on the KEGG database, pathway enrichment analysis of DEPs revealed that differential proteins between the control group and the CA treatment group were associated with 71 KEGG pathways. These KEGG pathways primarily encompass five categories: genetic information processing, cellular processes, human diseases, environmental information process-

Table 2. Analysis of Related DEPs

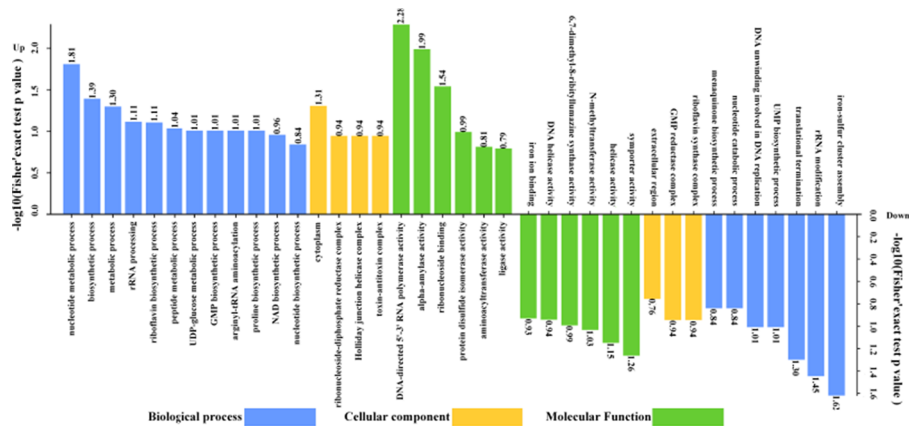
| accession | protein description | Log2FC | regulated type | p-value | gene name |
|--|---|--------------|----------------|-------------|------------------|
| cell wall and cell membrane | | | | | |
| Q931S1 | regulatory protein MsrR | -2.037636839 | down | 0.033417809 | msrR |
| A0A380E1E2 | cell division protein FtsI | -0.556133698 | down | 0.022516832 | ftsI_4 |
| A0A0H3KCB3 | cell division protein DivIB | -0.298043263 | down | 0.024976005 | ftsQ |
| A0A9N8HYT1 | FmtA protein involved in methicillin resistance affects cell wall cross-linking and amidation | -0.512859335 | down | 0.008532367 | fmtA_1 |
| A0A133Q0M9 | bacterial membrane protein YfhO | -0.607828221 | down | 0.043709012 | HMPREF3211_01286 |
| protein biosynthesis | | | | | |
| W8U3 × 2 | large ribosomal subunit proteins uL6 | 0.328922637 | up | 0.032038908 | rplF |
| A0A7R6NZR0 | large ribosomal subunit proteins bL27 | 0.793155053 | up | 0.034074057 | rpmA |
| A0A0E0VLH6 | large ribosomal subunit proteins uL11 | 0.345919858 | up | 0.046057472 | rplK |
| A6QJ60 | large ribosomal subunit proteins uL13 | 0.674079885 | up | 0.004877267 | rplM |
| A0A0E1VNP3 | large ribosomal subunit proteins uL18 | 0.591708397 | up | 0.018095062 | rplR |
| A0A6B3IL27 | small ribosomal subunit proteins uS4 | -1.253145593 | down | 0.040026194 | rpsD |
| A0A8D9S JL0 | small ribosomal subunit proteins uS8 | 0.469072316 | up | 0.028228659 | rpsH |
| A0A2S6DS24 | ribosome maturation factor RimM | 0.443484247 | up | 0.000320881 | rimM |
| A0A0E1VIS8 | peptidase propeptide and YPEB domain protein | 0.334494901 | up | 0.000970872 | HMPREF0776_2778 |
| DNA replication, nucleotide synthesis, and homeostasis correlation | | | | | |
| A0A7U4CHE4 | DNA-directed RNA polymerase subunit alpha | 0.577784015 | up | 0.001794672 | rpoA |
| A0A0E1VK28 | DNA-directed RNA polymerase subunit beta | 0.33181068 | up | 0.004594972 | rpoB |
| A0A9P2XZB2 | DNA-directed RNA polymerase subunit epsilon | 0.588068777 | up | 0.027553328 | rpoY |
| A0A0E0VP53 | transcription antitermination protein NusB | 0.386975115 | up | 0.017614548 | nusB |
| T1Y982 | global transcriptional regulator Spx | 0.467248229 | up | 0.049209555 | spx |
| A0A380DRT4 | molybdate-binding protein | -0.381006553 | down | 0.033648353 | modA |
| A0A133PU10 | nucleoside diphosphate kinase | -0.46147057 | down | 0.005338384 | ndk |
| A0A0U1MUK5 | ornithine carbamoyltransferase | -1.566646586 | down | 0.048956471 | argF |
| virulence-related factors | | | | | |
| A0A380EIU1 | exotoxin | -1.184833497 | down | 0.040785319 | NCTC10702_01843 |
| A0A075T6B6 | alpha-hemolysin (fragment) | -0.714771433 | down | 0.030968779 | hla |
| A0A380EP88 | leukocidin S subunit | -0.78373541 | down | 0.028088622 | lukS |
| A0A075T6B6 | type VII secretion system protein EssB | -0.680991563 | down | 0.011305551 | SAAG_00768 |
| A0A6G7K3 × 7 | methicillin-resistant protein (fragment) | -0.562911537 | down | 0.032503493 | mecA |
| A0A9Q3R710 | staphylococcal protein | -0.470996096 | down | 0.022521231 | E1948_09610 |
| other important DEPs | | | | | |
| A0A0H3K9Q0 | ArsR family transcriptional regulator | -1.323982071 | down | 0.030418578 | NWMN_2049 |
| A0A6M1XK70 | ATP-binding protein (Fragment) | 0.407863275 | up | 0.015965836 | G6Y24_03695 |
| A0A9N7S2L9 | methicillin resistance regulatory sensor-transducer MecR1 | -0.333962981 | down | 0.039950937 | mecR1 |
| A0A380DNQ9 | lysostaphin | 0.559739376 | up | 0.040176229 | lytM_2 |
| A0A7U7IC40 | capsular polysaccharide synthesis enzyme | 0.461922097 | up | 0.001129598 | capO |
| A0A0E7QLN2 | aerobactin siderophore biosynthesis protein | 0.275364205 | up | 0.004805085 | iucC_2 |

ing, and metabolism. In the metabolic pathway, DEPs are primarily involved in the biosynthesis of secondary metabolites. In the environmental information processing pathway, DEPs are primarily involved in a two-component system (TCS). In the genetic information processing pathway, DEPs are primarily associated with the ribosome. In the human diseases pathway, DEPs are primarily associated with *S. aureus* infection. In the cellular processes pathway, DEPs are primarily associated with quorum sensing (Figure 2B). Screening the top 20 pathways with the most significant enrichment of DEPs revealed that they were predominantly enriched in the glycolysis/gluconeogenesis pathway and the streptomycin biosynthesis pathway. More precisely, nine DEPs were found to be related to the glycolysis/gluconeogenesis route, while two DEPs were associated with the streptomycin biosynthesis pathway. Five DEPs were implicated in the TCA cycle, five DEPs were associated with aminoacyl-tRNA biosynthesis, and three DEPs were involved in teichoic acid biosynthesis. It is noteworthy that these KEGG pathways play a crucial role in

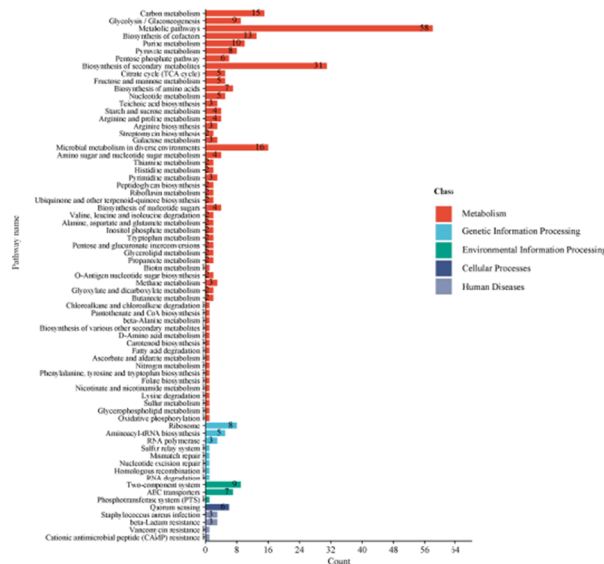
maintaining the cell wall stability. Moreover, DEPs were predominantly enriched in metabolic pathways, with 58 DEPs involved in metabolic pathways and nine DEPs implicated in the two-component signal system pathway (Figure 2C).

3.4. Protein–Protein Interaction (PPI) Network Analysis of DEPs

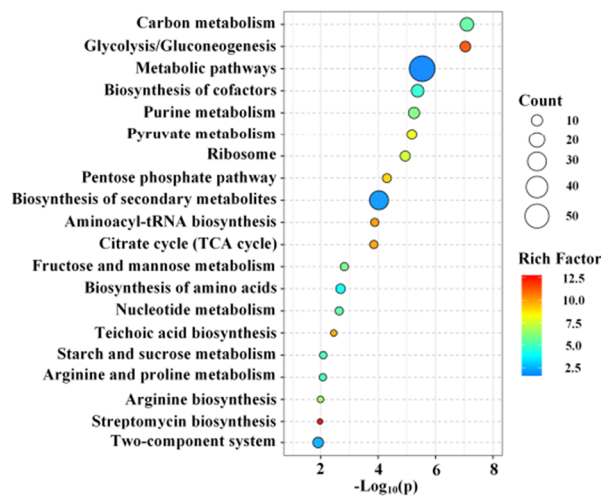
Analysis of the PPI network of DEPs in the control and CA treatment groups revealed that differential proteins involved in protein biosynthesis, DNA replication, nucleotide synthesis, and homeostasis exhibited a higher degree of interaction with their neighbors. Among these, five upregulated differential proteins related to protein biosynthesis (including RplF, RplK, RplM, RplR, RpsD, and RpsH) were part of the most complex network. The link between RpoB and RplR, RpsH, RpsD, and RplM suggests that proteins involved in protein biosynthesis may interact with processes related to nucleotide biosynthesis and DNA replication repair. Moreover, the association between MgrA and Hla, SdrD, and MecA indicates that



(A) GO enrichment analysis of DEPs



(B) KEGG enrichment analysis of DEPs



(C) KEGG pathway enrichment bubble diagram (top20) of DEPs

Figure 2. Enrichment Analysis of DEPs between the control group and the CA treatment group. Note: (A) Abscissa represents the GO functional category of the DEPs, and the ordinate represents the negative logarithmic transformation of the *p*-value. (B) Abscissa represents the number of DEPs, and the ordinate represents the KEGG enrichment pathways. (C) Abscissa represents the negative logarithmic transformation of the *p*-value, the ordinate represents the KEGG enrichment pathways, the circle color indicates the rich factor, and the circle size indicates the number of DEPs.

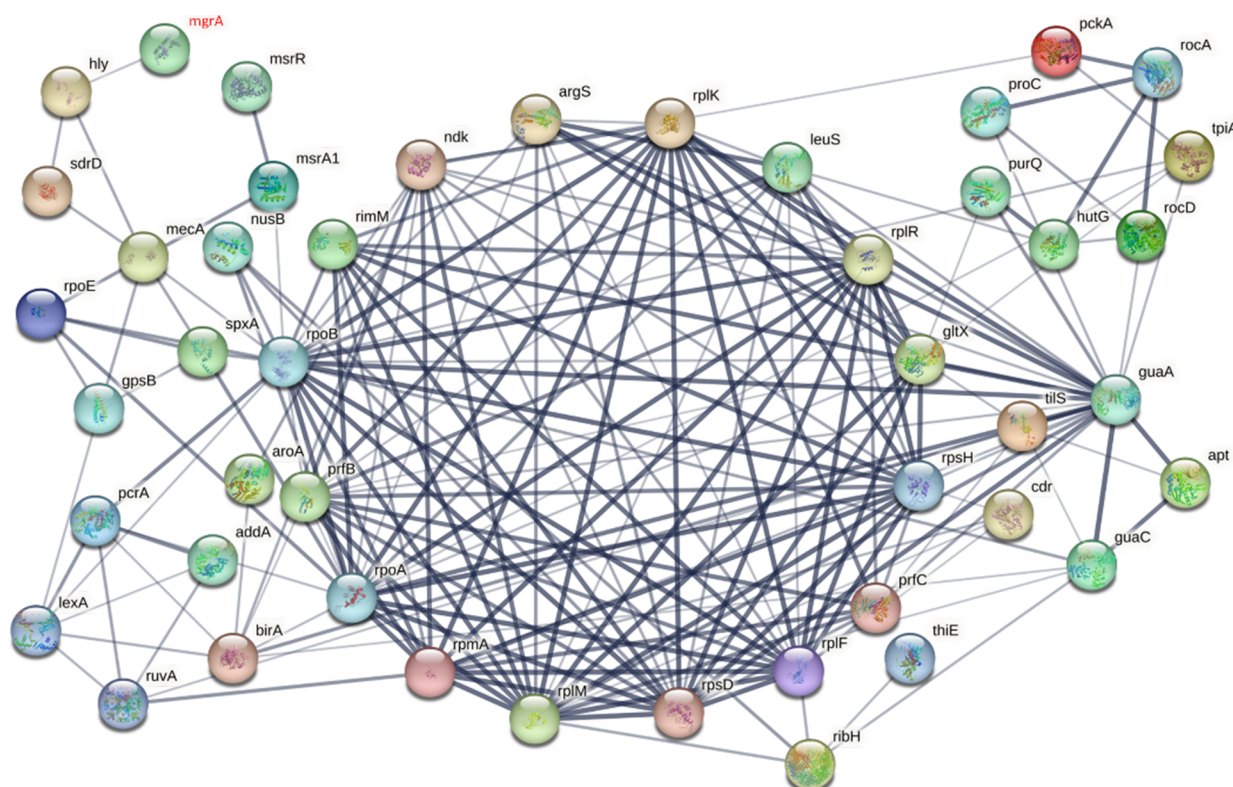


Figure 3. Analysis of the DEPs interaction network. Note: Nodes in the PPI network represent proteins, and the lines represent associations between two proteins.

MgrA plays a role in controlling the expression of the associated virulence factors in MRSA (Figure 3).

3.5. Effect of CA on the Expression of Recombinant Protein

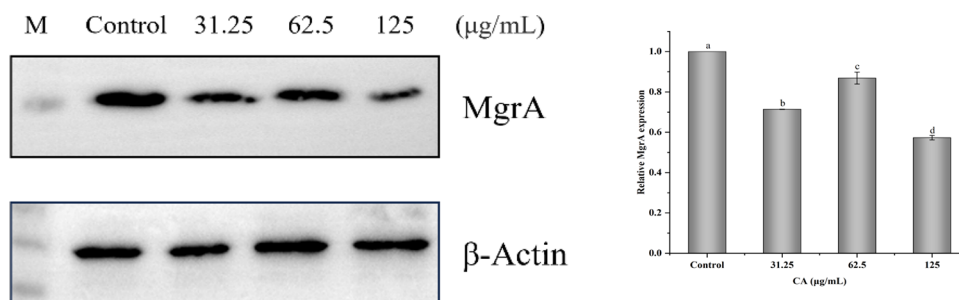
The results showed notable disparities in band thickness after exposure to CA and MRSA in comparison to those of the control group. Grayscale analysis was used to evaluate the effect of different doses of CA on the expression of MgrA protein in MRSA. The findings demonstrated that CA can significantly inhibit the expression of recombinant protein MgrA ($p < 0.05$) (Figure 4A). To further investigate the impact of CA on the transcriptional regulation of MgrA and its regulatory genes in MRSA, the mRNA transcription levels of *mgrA*, *hla*, *sdrD*, and *spa* genes were assessed using RT-qPCR. The results indicated that, compared to the control group, the transcription levels of *mgrA*, *hla*, and *sdrD* genes were significantly reduced following treatment with various concentrations of CA, decreasing by factors of 0.22, 0.38, and 0.61, respectively. In comparison with the control group, the transcriptional level of the *spa* gene was upregulated by a factor of 0.1 ($p < 0.05$) (Figure 4B). This observation aligns with the findings from proteomics sequencing, suggesting that CA can inhibit transcriptional regulation of MgrA in vitro. Furthermore, incubating CA with purified MgrA protein at various temperatures led to the observation of a notable reduction in the thermal stability of MgrA (Figure 4C). Thermostable migration assays demonstrated that CA can directly interact with MgrA, thus inhibiting its activity.

4. DISCUSSION

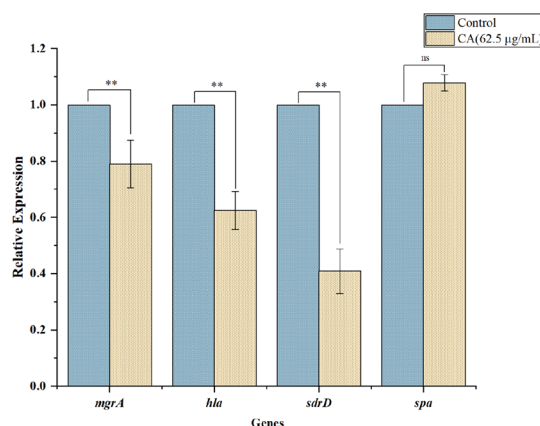
In this study, TMT quantitative proteomics was employed to reveal that CA exerts its antibacterial effects by altering the

structure and function of the MRSA cell wall and membrane as well as influencing DNA replication, nucleotide synthesis, homeostasis, and protein biosynthesis, while downregulating key virulence factors and drug resistance genes in MRSA.

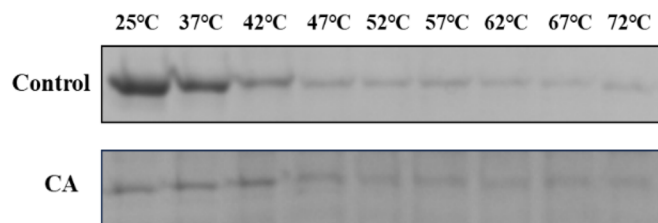
A single membrane comprising phosphatidylglycerol and cardiolipin encircles *S. aureus*, while it is enveloped by a robust cell wall primarily made up of peptidoglycan. Peptidoglycan is indispensable for the survival of cells. The cell wall plays a crucial role in supporting cell growth and basic physiological processes, serving as the essential framework of bacterial cells. The bacterial cell membrane plays a crucial role in several vital processes, such as selectively regulating the transport of nutrients and metabolites, maintaining proper internal osmotic pressure, and serving as an essential platform for the synthesis of the cell wall. The antibacterial effect of essential oils primarily involves their interaction with proteins and sterols present in the cell wall, leading to damage to the structure and function of the cell membrane, ultimately resulting in cell death.²¹ MsrR, a critical regulatory protein primarily present within the cell wall of Gram-positive bacteria, is categorized as being within the LytR-CpsA-Psr family of transcriptional attenuators associated with the cell membrane. Cell wall active agents, including β -lactams, glycopeptides, and lysostaphin, are known inducers of MsrR, which plays a significant role in conferring methicillin resistance in *S. aureus*. MsrR is involved in the maintenance of the cell membrane, cell separation, and the pathogenicity of *S. aureus*.²² Following CA treatment, the activity of MsrR was notably inhibited by a factor of 2.04, suggesting that CA impedes the growth and proliferation of MRSA by targeting key regulatory factors in the cell wall membrane. The fusion of the cell membrane and the cell wall layer during bacterial cytoplasmic division necessitates the



(A) The western blot analysis of MgrA protein



(B) The effect of CA on the transcriptional level of MgrA-regulated genes



(C) The effect of CA on the activity of MgrA protein

Figure 4. Effect of CA on the expression of recombinant protein. Note: (A) Abscissa represents the concentration of CA, and the ordinate represents the relative expression of the MgrA protein. (B) Abscissa represents the genes, and the ordinate represents the relative expression of the genes. (C) Changes of MgrA protein activity in the control group and CA treatment group under different temperatures.

coordination of numerous proteins, forming a complex multiprotein assembly. FtsI (PBP3) is an essential penicillin-binding protein (PBP) involved in cell division. The FtsWI complex, composed of FtsI and FtsW, serves as a critical transpeptidase in peptidoglycan synthesis. Both types of peptidoglycan synthases are believed to participate in the biological process of synthesizing peptidoglycan layers.²³ DivIB is a membrane protein that has two functional sites. It consists of a short cytoplasmic N-terminal domain (Cyto), a transmembrane (TM) segment, and a large extracellular portion that is 24 kDa in size. Both the transmembrane protein DivIB and its counterpart FtsQ are essential components of the bacterial divisome, playing a crucial role in the production of peptidoglycan layers.²⁴ After CA treatment of MRSA, FtsI protein was downregulated by 0.57-fold and DivIB protein by 0.30-fold. FmtA, functioning as a penicillin recognition protein (PRP), exhibits hydrolytic activity, participating in the formation of ester linkages between D-Ala and wall teichoic acid (WTA) skeletons within the cell wall of *S. aureus*.²⁵

Lysostaphin is among the most potent antibacterial compounds found in nature, exhibiting endopeptidase activity against common *S. aureus* strains (including MRSA) as well as coagulase-positive and coagulase-negative pathogens. By hydrolyzing the pentaglycine cross-bridge within the peptidoglycan of the *S. aureus* cell wall, lysostaphin enables the swift lysis of both planktonic bacteria and biofilms.²⁶ In this study, following CA treatment of MRSA, FmtA protein was downregulated by 0.51-fold, while lysostaphin was upregulated by 0.56-fold. These findings indicate that CA interferes with the composition of the cell wall and the cell membrane by blocking the production of peptidoglycan in the MRSA cell wall. This leads to the destruction or deactivation of the cell.

The ribosome serves as a molecular machinery for protein synthesis in cells. It participates in the process of translating RNA into a protein. It comprises two ribosomal subunits of varying sizes, both of which are essential for translation. During protein synthesis, the ribosomal 30S small subunit and the 50S large subunit collaborate synergistically to translate mRNA

into polypeptide chains. RimM is a vital auxiliary protein pivotal for the ultimate stage of assembling the ribosomal 30S small subunit, primarily accountable for its assembly and organization.⁵ In this study, RimM was upregulated by a factor of 0.44 following CA treatment of MRSA, suggesting that CA can enhance the binding of small ribosomal subunits to mRNA, thereby safeguarding bacterial protein synthesis. In addition, after CA treatment, the ribosomal large subunit proteins uL6, bL27, uL11, uL13, and uL18 were upregulated by 0.33-fold, 0.79-fold, 0.35-fold, 0.67-fold, and 0.59-fold, respectively. All of these proteins are involved in the cell metabolism process of ribosomal protein production, suggesting that CA may enhance ribosomal subunit aggregation and expedite protein synthesis, ensuring continuous protein production.

Transcription in all life forms is mediated by the DNA-dependent RNA polymerase (RNAP). The core RNAP consists of two α subunits, one β subunit, and one β' subunit. Additionally, smaller subunits such as δ , δ' , and ω are essential for supporting the transcription process in Gram-positive bacteria.²⁷ The study results revealed that DNA-directed RNA polymerase subunit α was upregulated by a factor of 0.58, DNA-directed RNA polymerase subunit β by a factor of 0.33, and DNA-directed RNA polymerase subunit ϵ by a factor of 0.59 after CA treatment. Spx global transcriptional regulators are pivotal in *S. aureus* for growth, general stress protection, and biofilm formation. Studies have shown that Spx can directly interact with the DNA-directed RNA polymerase subunit α , thereby controlling global transcription initiation through a distinct mechanism.²⁸ These findings suggest that DNA replication in *S. aureus* cells is inhibited, leading the bacteria to activate proteins involved in DNA replication and repair to sustain normal growth, metabolism, and homeostasis.

ABC transporters make up a crucial protein family in prokaryotes. Genomic research revealed that ABC transporters make up approximately 5% of the genomes in *Escherichia coli* and *Bacillus subtilis*, underscoring the vital role of ABC transporters in both Gram-positive and Gram-negative bacteria. ABC transporters facilitate the transportation of various substances, such as metal ions and proteins, across cell membranes in a one-way path by using ATP hydrolysis.²⁹ Bacterial ABC transporters are pivotal in facilitating numerous cellular processes, such as multidrug resistance (MDR), nutrient acquisition, spore formation, conjugation, biofilm development, and toxin secretion.³⁰ Following CA treatment, the expression of the ABC transporter ATP-binding protein (fragment) was upregulated by a factor of 0.41. Additionally, after CA treatment of MRSA in this study, the methicillin-resistant protein (fragment) and methicillin-resistant regulatory sensor-transducer MecR1 were downregulated by factors of 0.56 and 0.33, respectively. The level of resistance to methicillin is strongly associated with the existence of the *mecA* gene, which is responsible for producing the penicillin-binding protein PBP2a. Methicillin-sensitive *Staphylococcus aureus* (MSSA) does not express the PBP2a protein due to regulation by the intracellular signaling pathway MecR1-MecI-MecA. MecR1, the *mecR1* gene product, serves as a transmembrane signaling protein, responding to β -lactam antibiotics, while MecI, encoded by the *mecI* gene, functions as a repressor protein upon exposure to extracellular β -lactam antibiotics. MecR1 undergoes a conformational change that activates its integrated membrane metalloproteinase domain, leading to the specific cleavage of MecI.³¹ Therefore, inhibiting the

expression of MecR1 may present a novel approach to reversing the antibiotic resistance of MRSA.

The KEGG enrichment analysis indicated that the proteins exhibiting differential expression were enriched in the pathway linked to *S. aureus* infection following CA treatment. *S. aureus* is a prominent foodborne pathogen and a primary causative agent of mastitis in ruminants. Usually, this microorganism generates a range of extracellular toxins, including Toxic Shock Syndrome Toxin-1 (TSST-1), epidermal exfoliative toxin, staphylococcal enterotoxin (SE), hemolysin, and leukocidin. Exotoxins released by *S. aureus* are essential contributors to the development of skin infections and mastitis. The leukocidin S subunit comprises two components, staphylococcal exotoxin S and F subunits (protein monomers). The binding of this subunit to the cell membrane of white blood cells results in the creation of transmembrane pores, leading to the subsequent lysis of the cells.³² Alpha-hemolysin (Hla) is a pore-forming toxin produced by most *S. aureus* isolates at the same time. The pathophysiology of *S. aureus* infections includes its crucial role in illnesses such as skin and soft tissue infections, pneumonia, and life-threatening peritonitis.³³ In addition, *S. aureus* has the capacity to produce numerous virulence factors, aiding in its evasion of the host's immune defenses and facilitating microbial colonization within the mammary tissues of animals³⁴; for instance, the virulence of *S. aureus* relies significantly on the Ess/VII protein secretion system, which is primarily dependent on four core membrane proteins: EssA, EssB, EssC, and EsaA.³⁵ Nucleoside diphosphate kinase (NDK) is a highly conserved multifunctional protein encoded by the *ndk* gene. It acts as a nucleotide metabolic enzyme. It regulates bacterial pathogenicity by controlling the generation and activation of substances outside the cell, regulating the T3SS system, modulating the QS system, and impacting the host's ability to adapt to germs.³⁶ The findings of this investigation indicated a notable decrease in the expression of Exotoxin by 1.18-fold following CA treatment, Leukocidin S subunit by 0.87-fold, Alpha-hemolysin (Fragment) by 0.71-fold, Type VII secretion system protein EssB by 0.68-fold, and Staphylococcal protein by 0.47-fold. Methicillin-resistant protein (Fragment) was downregulated by 0.56-fold, and NDK protein was downregulated by 0.46-fold, indicating that CA exerts its antibacterial activity by inhibiting the production of *Staphylococcus aureus*-related toxin proteins.

Furthermore, studies suggest that the main antibacterial action of CA primarily involves its ability to disrupt microbial cell membranes, cell walls, and internal targets, including proteins, DNA, and RNA. As a key global regulatory transcription factor in *S. aureus*, MgrA regulates the expression of numerous virulence genes within the *S. aureus* genome, significantly contributing to the pathogenesis of *S. aureus* infections. This regulation impacts various biological characteristics of *S. aureus*, including growth, metabolism, antibiotic resistance, and immune system.³⁷ Studies have demonstrated that MgrA governs the expression of Hla and Spa through a dual mechanism. The first involves a Agr-dependent pathway, while the second operates via a Agr-independent pathway, which triggers Hla activation by directly interacting with its promoter. The expression of Hla is also regulated by the staphylococcal accessory element Sae.^{38,39} Additionally, MgrA has the capability to influence the metabolic pathway of *S. aureus*, particularly in regulating the glycolysis pathway, which holds significance in the adaptability of *S. aureus* across diverse environments. Elevated MgrA expression enhances the

resistance of *S. aureus* to multiple antibiotics. In recent years, research has focused on MgrA inhibitors. For example, some small molecule compounds such as salicylidene acylhydrazides and lopinavir have been shown to inhibit MgrA function. Although CA exerts antibacterial effects mainly by destroying bacterial cell membranes, it is also a natural antibacterial agent with additional intracellular targets. CA has the ability to bind to proteins and inhibit nucleic acid and protein synthesis.⁴⁰ For deeper exploration of CA's impact on MgrA protein function in MRSA, we induced MgrA protein expression and obtained purified antibody. Western blot analysis revealed that CA inhibited MgrA protein expression in a dose-dependent manner, and RT-qPCR results demonstrated that CA significantly inhibited the transcription levels of the *mgrA*, *hla*, *spa*, and *sdrD* genes. Additionally, the effect of CA on MgrA protein was further confirmed using this study's thermal stable migration method. Therefore, future research should focus on discovering and designing MgrA inhibitors to find more efficient, selective, and specific inhibitors, thereby providing more effective treatment options for *S. aureus* infections. The data analysis of this study shows that the mechanism of CA in MRSA is mainly related to cell walls, cell membranes, RNA, and protein biosynthesis. It is worth noting that the current research is carried out only at the protein level, and further experiments are needed to clarify the mechanism of CA in MRSA.

5. CONCLUSIONS

In this study, TMT quantitative proteomics was used to analyze the changes in protein expression in MRSA induced by CA, thereby elucidating the antibacterial mechanism of CA against MRSA. A total of 254 DEPs were identified following CA treatment, with 161 upregulated and 93 downregulated. These DEPs comprehensively revealed the antibacterial mechanism of CA against MRSA. DEPs related to nucleotide synthesis, homeostasis, and protein biosynthesis were significantly upregulated, while DEPs involved in the cell wall, cell membrane, and virulence factors were significantly downregulated. Thermostable migration assays demonstrated that CA directly interacts with the MgrA protein, inhibiting its activity, significantly suppressing the expression of recombinant MgrA protein, and reducing the transcription levels of *mgrA*, *hla*, and *sdrD* genes. These results offer a more effective strategy for the treatment of MRSA infections using natural plant extracts and provide a theoretical basis for preventing MRSA tolerance to antibiotics.

■ ASSOCIATED CONTENT

Data Availability Statement

The mass spectrometry data have been deposited to the Proteome Xchange Consortium (<https://proteomecentral.proteomexchange.org>) via the PRIDE partner repository with the data set identifier PXD054851.

SI Supporting Information

The Supporting Information is available free of charge at <https://pubs.acs.org/doi/10.1021/acs.jproteome.4c00520>.

15% SDS-PAGE gel electrophoresis (PDF)

Total number of peptides identified in all of the samples, total number of proteins identified in all of the samples, total number of DEPs identified in both the control group and the CA treatment group, and all DEPs GO enrichment annotation (ZIP)

■ AUTHOR INFORMATION

Corresponding Author

Guiqin Wang – College of Animal Science and Technology, Ningxia University, Yinchuan 750021, China; orcid.org/0009-0005-8806-3851; Email: nxwgq@126.com

Authors

Xiaohui Chen – College of Animal Science and Technology, Ningxia University, Yinchuan 750021, China

Panpan Liu – College of Animal Science and Technology, Ningxia University, Yinchuan 750021, China

Jingge Wang – College of Animal Science and Technology, Ningxia University, Yinchuan 750021, China

Xiaoqiang He – College of Animal Science and Technology, Ningxia University, Yinchuan 750021, China

Jianchong Wang – College of Animal Science and Technology, Ningxia University, Yinchuan 750021, China

Haorong Chen – College of Animal Science and Technology, Ningxia University, Yinchuan 750021, China

Complete contact information is available at:

<https://pubs.acs.org/10.1021/acs.jproteome.4c00520>

Author Contributions

X.C.: conceptualization, methodology, and writing-original draft. P.L. and J.W.: visualization and investigation. X.H. and J.W.: visualization and investigation. H.C.: supervision. G.W.: writing-review and editing.

Funding

This work was supported by the National Natural Science Foundation of China (32160852). Thanks to all the teachers and students who have contributed to this paper. We thank Shanghai Bioprofile Technology Company Ltd. for technological assistance in TMT quantitative proteomics experiment.

Notes

The authors declare no competing financial interest.

■ REFERENCES

- (1) Martins, L.; Barcelos, M. M.; Cue, R. I.; Anderson, K. L.; dos Santos, M. V.; Gonçalves, J. L. Chronic subclinical mastitis reduces milk and components yield at the cow level. *J. Dairy Res.* **2020**, *87* (3), 298–305.
- (2) Lacombe, A.; Mcgivney, C.; Tadepalli, S.; Sun, X. H.; Wu, V. C. H. The effect of American cranberry (*Vaccinium macrocarpon*) constituents on the growth inhibition, membrane integrity, and injury of *Escherichia coli* O157:H7 and *Listeria monocytogenes* in comparison to *Lactobacillus rhamnosus*. *Food Microbiol.* **2013**, *34* (2), 352–359.
- (3) Hillerton, J. E.; Kliem, K. E. Effective treatment of *Streptococcus uberis* clinical mastitis to minimize the use of antibiotics. *J. Dairy Sci.* **2002**, *85* (4), 1009–1014.
- (4) Rajamanickam, K.; Yang, J.; Sakharkar, M. K. Phytochemicals as alternatives to antibiotics against major pathogens involved in bovine respiratory disease (BRD) and bovine mastitis (BM). *Bioinformation.* **2019**, *15* (1), 32–35.
- (5) Deng, H. T.; Xue, B.; Wang, M. Y.; Tong, Y. Q.; Tan, C.; Wan, M. Z.; Kong, Y. W.; Meng, X. J.; Zhu, J. Y. TMT-Based quantitative proteomics analyses reveal the antibacterial mechanisms of anthocyanins from *Aronia melanocarpa* against *Escherichia coli* O157:H7. *J. Agric. Food Chem.* **2022**, *70* (26), 8032–8042.
- (6) Li, Y. X.; Erhunmwunsee, F.; Liu, M.; Yang, K. L.; Zheng, W. F.; Tian, J. Antimicrobial mechanisms of spice essential oils and application in food industry. *Food Chem.* **2022**, *382*, No. 132312.
- (7) Tariq, S.; Wani, S.; Rasool, W.; Shafi, K.; Bhat, M. A.; Prabhakar, A.; Shalla, A. H.; Rather, M. A. A comprehensive review of the

antibacterial, antifungal and antiviral potential of essential oils and their chemical constituents against drug-resistant microbial pathogens. *Microb. Pathogen*. **2019**, *134*, No. 103580.

(8) Gill, A. O.; Holley, R. A. Disruption of *Escherichia coli*, *Listeria monocytogenes* and *Lactobacillus sakei* cellular membranes by plant oil aromatics. *Int. J. Food Microbiol.* **2006**, *108* (1), 1–9.

(9) Turina, A. V.; Nolan, M. V.; Zygadlo, J. A.; Perillo, M. A. Natural terpenes: self-assembly and membrane partitioning. *Biophys. Chem.* **2006**, *122* (2), 101–113.

(10) Wang, L. H.; Wang, M. S.; Zeng, X. A.; Gong, D. M.; Huang, Y. B. An in vitro investigation of the inhibitory mechanism of β -galactosidase by cinnamaldehyde alone and in combination with carvacrol and thymol. *Biochim Biophys Acta Gen Subj.* **2017**, *1861* (1), 3189–3198.

(11) Usai, F.; Sotto, A. D. *trans*-cinnamaldehyde as a novel candidate to overcome bacterial resistance: an overview of in vitro studies. *Antibiotics (Basel)* **2023**, *12* (2), 254.

(12) Yemis, G. P.; Delaquis, P. Natural compounds with antibacterial activity against *Cronobacter* spp. in powdered infant formula: a review. *Front. Nutr.* **2020**, *7*, No. 595964.

(13) Chen, X. H.; Liu, P. P.; Luo, X. F.; Huang, A. L.; Wang, G. Q. Study on the antibacterial activity and mechanism of Cinnamaldehyde against Methicillin-resistant *Staphylococcus aureus*. *Eur. Food Res. Technol.* **2024**, *250* (4), 1069–1081.

(14) Zhu, H. M.; Du, M.; Fox, L.; Zhu, M. J. Bactericidal effects of Cinnamon cassia oil against bovine mastitis bacterial pathogens. *Food Control* **2016**, *66*, 291–299.

(15) Abd El-Aziz, N. K.; Ammar, A. M.; El-Naenaeey, E. Y. M.; El Damaty, H. M.; Elazazy, A. A.; Hefny, A. A.; Shaker, A.; Eldesoukey, I. E. Antimicrobial and antibiofilm potentials of cinnamon oil and silver nanoparticles against *Streptococcus agalactiae* isolated from bovine mastitis: new avenues for countering resistance. *BMC Vet. Res.* **2021**, *17* (1), 136.

(16) Bedoya-Serna, C. M.; Dacanal, G. C.; Fernandes, A. M.; Pinho, S. C. Antifungal activity of nanoemulsions encapsulating oregano (*Origanum vulgare*) essential oil: in vitro study and application in Minas Padrao cheese. *Braz. J. Microbiol.* **2018**, *49* (4), 929–935.

(17) Jia, S. L.; Hong, H.; Yang, Q. F.; Liu, X. C.; Zhuang, S.; Li, Y.; Liu, J.; Luo, Y. K. TMT-based proteomic analysis of the fish-borne spoiler *Pseudomonas psychrophila* subjected to chitosan oligosaccharides in fish juice system. *Food Microbiol.* **2020**, *90*, No. 103494.

(18) Du, G. F.; Yin, X. F.; Yang, D. H.; He, Q. Y.; Sun, X. S. Proteomic investigation of the antibacterial mechanism of *trans*-Cinnamaldehyde against *Escherichia coli*. *J. Proteome Res.* **2021**, *20* (5), 2319–2328.

(19) Fan, Q. X.; Dong, X. R.; Wang, Z. W.; Yue, Y.; Yuan, Y. H.; Wang, Z. L.; Yue, T. L. TMT-Based quantitative proteomics and non-targeted metabolomic analyses reveal the antibacterial mechanism of Hexanal against *Vibrio parahaemolyticus*. *J. Agric. Food. Chem.* **2023**, *71* (31), 12105–12115.

(20) Yang, L. B.; Guo, G.; Tian, Z. Q.; Zhou, L. X.; Zhu, L. J.; Peng, J.; Sun, C. Q.; Huang, M. J. TMT-based quantitative proteomic analysis of the effects of novel antimicrobial peptide AMP-17 against *Candida albicans*. *J. Proteomics* **2022**, *250*, No. 104385.

(21) Ahmad, A.; Viljoen, A. The in vitro antimicrobial activity of *Cymbopogon* essential oil (lemon grass) and its interaction with silver ions. *Phytomedicine* **2015**, *22* (6), 657–665.

(22) Rossi, J.; Bischoff, M.; Wada, A.; Berger-Bächli, B. MsrR, a putative cell envelope-associated element involved in *Staphylococcus aureus sarA* attenuation. *Antimicrob. Agents Chemother.* **2003**, *47* (8), 2558–2564.

(23) Marmont, L. S.; Bernhardt, T. G. A conserved subcomplex within the bacterial cytokinetic ring activates cell wall synthesis by the FtsW-FtsI synthase. *Proc. Natl. Acad. Sci. U. S. A.* **2020**, *117* (38), 23879–23885.

(24) Bottomley, A. L.; Kabli, A. F.; Hurd, A. F.; Turner, R. D.; Garcia-Lara, J.; Foster, S. J. *Staphylococcus aureus* DivIB is a peptidoglycan-binding protein that is required for a morphological checkpoint in cell division. *Mol. Microbiol.* **2014**, *94* (5), 1041–1064.

(25) Dalal, V.; Dhankhar, P.; Singh, V.; Singh, V.; Rakhminov, G.; Golemi-Kotra, D.; Kumar, P. Structure-based identification of potential drugs against FmtA of *Staphylococcus aureus*: virtual screening, molecular dynamics, MM-GBSA, and QM/MM. *Protein J.* **2021**, *40* (2), 148–165.

(26) Zha, J.; Li, J. Y.; Su, Z.; Akimbekov, N.; Wu, X. Lysostaphin: engineering and potentiation toward better applications. *J. Agric. Food. Chem.* **2022**, *70* (37), 11441–11457.

(27) Mao, C. Y.; Zhu, Y.; Lu, P.; Feng, L. P.; Chen, S. Y.; Hu, Y. B. Association of ω with the C-Terminal region of the β' subunit is essential for assembly of RNA polymerase in *Mycobacterium tuberculosis*. *J. Bacteriol.* **2018**, *200* (12), No. e00159-18.

(28) Pamp, S. J.; Frees, D.; Engelmann, S.; Hecker, M.; Ingmer, H. Spx is a global effector impacting stress tolerance and biofilm formation in *Staphylococcus aureus*. *J. Bacteriol.* **2006**, *188* (13), 4861–4870.

(29) Akhtar, A. A.; Turner, D. P. J. The role of bacterial ATP-binding cassette (ABC) transporters in pathogenesis and virulence: Therapeutic and vaccine potential. *Microb. Pathogen.* **2022**, *171*, No. 105734.

(30) Basavanna, S.; Khandavilli, S.; Yuste, J.; Cohen, J. M.; Hosie, A. H. F.; Webb, A. J.; Thomas, G. H.; Brown, J. S. Screening of *Streptococcus pneumoniae* ABC transporter mutants demonstrates that LivJ/HMGF, a branched-chain amino acid ABC transporter, is necessary for disease pathogenesis. *Infect. Immun.* **2009**, *77* (8), 3412–3423.

(31) Belluzo, B. S.; Abriata, L. A.; Giannini, E.; Mihovilcevic, D.; Dal Peraro, M.; Llarrull, L. I. An experiment-informed signal transduction model for the role of the *Staphylococcus aureus* MecR1 protein in β -lactam resistance. *Sci. Rep.* **2019**, *9* (1), 19558.

(32) Bownik, A. In vitro effects of staphylococcal leukocidin LukE/LukD on the proliferative ability of lymphocytes isolated from common carp (*Cyprinus carpio* L.). *Fish Shellfish Immunol.* **2006**, *20* (4), 656–659.

(33) Adhikari, R. P.; Thompson, C. D.; Aman, M. J.; Lee, J. C. Protective efficacy of a novel alpha hemolysin subunit vaccine (AT62) against *Staphylococcus aureus* skin and soft tissue infections. *Vaccine* **2016**, *34* (50), 6402–6407.

(34) Abril, A. G.; Villa, T. G.; Barros-Velázquez, J.; Cañas, B.; Sánchez-Pérez, A.; Calo-Mata, P.; Carrera, M. *Staphylococcus aureus* exotoxins and their detection in the dairy industry and mastitis. *Toxins (Basel)* **2020**, *12* (9), 537.

(35) Jäger, F.; Zoltner, M.; Kneuper, H.; Hunter, W. N.; Palmer, T. Membrane interactions and self-association of components of the Ess/Type VII secretion system of *Staphylococcus aureus*. *FEBS Lett.* **2016**, *590* (3), 349–357.

(36) Zhang, L.; Song, M. F.; Yang, N.; Zhang, X. W.; Raza, S. H. A.; Jia, K. X.; Tian, J. X.; Zhang, Y.; Zhang, D. X.; Shi, Q. M.; Wu, T. L.; Kang, Y. H.; Hou, G. X.; Qian, A. D.; Wang, G. Q.; Shan, X. F. Nucleoside Diphosphate Kinases (*ndk*) reveals a key role in adhesion and virulence of *Aeromonas veronii*. *Microb. Pathog.* **2020**, *149*, No. 104577.

(37) Crosby, H. A.; Schlievert, P. M.; Merriman, J. A.; King, J. M.; Salgado-Pabón, W.; Horswill, A. R. The *Staphylococcus aureus* global regulator MgrA modulates clumping and virulence by controlling surface protein expression. *PLoS Pathog.* **2016**, *12* (5), No. e1005604.

(38) Mcadow, M.; Missiakas, D. M.; Schneewind, O. *Staphylococcus aureus* secretes coagulase and von Willebrand factor binding protein to modify the coagulation cascade and establish host infections. *J. Innate Immun.* **2012**, *4* (2), 141–148.

(39) Lei, M. G.; Lee, C. Y. MgrA Activates *Staphylococcal* capsule via sigA-dependent promoter. *J. Bacteriol.* **2020**, *203* (2), No. e00495-20.

(40) Visvalingam, J.; Hernandez-Doria, J. D.; Holley, R. A. Examination of the genome-wide transcriptional response of *Escherichia coli* O157:H7 to cinnamaldehyde exposure. *Appl. Environ. Microbiol.* **2013**, *79* (3), 942–950.